Available online at www.sciencedirect.com
ScienceDirect
Ceramics International 37 (2011) 377–385
CERAMICS INTERNATIONAL
www.elsevier.com/locate/ceramint

Ash from sunflower husk as raw material for ceramic products

Nancy Quaranta [a,1,*], Miguel Unsen [a], Hugo López [a], Claudio Giansiracusa [a], Judith A. Roether [b,2], Aldo R. Boccaccini [b,2]

[a] Grupo de Estudios Ambientales – GEA, Facultad Regional San Nicolás, Universidad Tecnológica Nacional, Colón 332, 2900 San Nicolás, Argentina
[b] Department of Materials, Imperial College London, London SW7 2AZ, UK

Received 2 July 2010; received in revised form 13 July 2010; accepted 2 September 2010
Available online 29 September 2010

Abstract

The objective of the present work was to characterize a residual material (ash) from edible oil industrial production and to study its feasibility as a starting material for fabrication of ceramics for the construction industry. The characterization of the ash was carried out by a range of techniques, such as humidity content measurement, particle size distribution analysis, weight loss on calcination, scanning electron microscopy and chemical composition analysis by X-ray dispersion energy and X-ray diffraction. The ash was compacted without other additions into ''green bodies'', which were treated at different temperatures in order to determine the sintering behaviour, and the occurrence of possible chemical reactions at the processing temperatures. From the experimental results and the analysis of the equilibrium diagrams of the major oxides present, the theoretical sintering temperatures were determined to be too high for an attractive cost-effective industrial scale process. Therefore new mixtures were designed adding different contents of milled discarded (cullet) glass to the ash in order to lower the working temperature. Final sintered products containing 30%, 40% and 50% of ash were produced which exhibit adequate properties for their use as ceramic products with a typology of lightening bricks.

Keywords: Sunflower ash; Bricks; Recycling; Cullet; Wastes management

1. Introduction

Industrial production of vegetable oil generates a large amount of waste during the entire production process, including the husks of the seeds used as raw material.

In the case of sunflower seeds, for example, they are introduced in a first stage into a process of grinding and hulled. Then, the nuggets with a small volume of shells, necessary to achieve an adequate protein content, are derived to the production of oil by pressing. This process produces the oil but also a residue that still contains high percentages of oil. This residue is conducted to a process of solvent extraction, which removes the remaining oil and creates a by-product that is intended to feed animals.

In the industrial oil manufacturing plant considered in this work, located in Santa Fe Province, Argentina, the greater volume of the shell product from the milling of the initial raw material is used directly as a boiler fuel, generating ash that accumulates in the base of the boiler. This ash, which is produced in quantities of 100–150 tons over periods of approximately 2 months, is employed currently in land-filling and road construction.

Numerous research studies have been carried out analyzing the pyrolysis and firing processes of natural organic wastes as a renewable and environmentally friendly energy source [1–3]. Biomass firing for heat and power production is being widely studied from the energetic exploitation point of view. Vine shoot, cherry and olive stones, coffee press cakes, tomato plant wastes, almond, nut and coconut husks, are some of the residues that have been used as bio-fuels [1–7]. While the environmental aspects of these processes are considered in relation to gas phase emissions, liquid phase effluents and solid residual materials, these last named wastes (solid residues) are not usually considered from the point of view of the feasibility of their recycling or reuse. Only the possibility of using them as adsorbents for remediation of water or industrial liquid effluents has been mentioned [8,9].

* Corresponding author at: Grupo de Estudios Ambientales – GEA, Facultad Regional San Nicolás, Universidad Tecnológica Nacional, Colón 332, 2900 San Nicolás, Argentina. Tel.: +54 3461 420820; fax: +54 3461 420820.
E-mail address: nquaranta@frsn.utn.edu.ar (N. Quaranta).
[1] CIC Researcher.
[2] Present address: Department of Materials Science and Engineering, University of Erlangen, Nuremberg, Germany.

0272-8842/$36.00 © 2010 Published by Elsevier Ltd and Techna Group S.r.l.
doi:10.1016/j.ceramint.2010.09.015

On the other hand, ashes generated as residues of industrial combustion processes of mineral materials such as coal, have been tested for various uses, mainly in the construction industry, in materials such as glass–ceramics, cement and concrete, and as filling material for roads, pavement construction as well as for restoration of soil [10–18].

The use of industrial ashes for levelling soil is a common practice and often not controlled, based on the fact that combustion ashes do not contain hazardous elements such as heavy metals. However, these materials can have compositions and properties that can cause significant changes in the physicochemical characteristics of soils, so that it is imperative to characterize them before their use in land-filling. Moreover, a thermal heat treatment of the ashes in form of powder compacts can lead to solid ceramic materials with enough structural integrity for use in the building industry [16–18].

This paper aims to investigate for the first time the development of novel sintered ceramic materials from the ash generated during burning husks of sunflower seeds, which is a waste being accumulated in a vegetable oil manufacturing plant. A complete characterization of the ash was carried out and the link between ash characteristics and final product properties was investigated.

2. Materials and methods

2.1. Ash characterization

Ash samples used for characterization were obtained from different sectors of the deposits located inside the industrial plant (Santa Fe, Argentina) in order to get samples as representative as possible of the totality of the material being accumulated.

A morphological study of the ash by scanning electron microscopy (SEM) using a Philips 505 instrument was performed. The chemical composition of the ash was determined by the X-ray energy dispersion (EDS) method.

The humidity content of ashes was determined by heat treatment of given amounts of ash in an electric furnace until constant weight was reached at a temperature of 100 °C. Weight loss by calcination was carried out on ash samples of grain size <600 μm at 800 °C for 3 h. The particle size distribution was determined by the method of sieving (ASTM C 92-76). Two different tests were carried out, one with the ashes containing humidity, as extracted from deposits, and the other with dry ash treated at 100 °C for 24 h.

Selected powdered samples were heat treated between 1300 and 1600 °C and were analyzed by X-ray diffraction (XRD), using a Philips PW 1390 instrument, with CuK-α radiation and Ni filter. The operating conditions were 40 kV, 20 mA and scanning speed of 1°/min.

2.2. Preparation and characterization of compact bodies

Green compacts were obtained by uniaxial compaction of ashes previously calcined, which acquired a characteristic powdery morphology with a humidity addition of between 5% and 9% as needed, using a compaction pressure of 100 MPa. Compacts of 70 mm × 40 mm and 10 mm in height were obtained.

The initial mixing was conducted with the following size distribution (p: particle size): 50% of coarse particles (212 μm > p > 150 μm), 30% of medium size particle (150 μm > p > 75 μm) and 20% of fine particles (p < 75 μm). Based on the results of the initial characterization of the material, in a parallel experiment mixtures were also prepared replacing coarse particles of ash for milled discarded (cullet) glass (p < 75 μm). The glass contents in the samples were (wt%): 30%, 40% and 50%.

Powder compacts were formed and heat-treated at temperatures in the range 1000–1400 °C in order to determine the sintering temperature of the mixtures.

The compacts produced were characterized using traditional techniques for such materials: optical and scanning electron microscopy (OM and SEM, respectively), chemical analysis by EDS, Vickers microhardness and permanent linear expansion measurements. The Vickers microhardness analysis was performed with a Shimatzu HMV2000 equipment. The optical microscopy analyses were made with a Zeiss-Axiotech microscope, with an annexed Donpisha 3CCD camera and image digitizer.

3. Results and discussion

The analysis of the morphology of the ash particles by SEM (Fig. 1) shows the presence of very small particles of size of a few microns, and clusters of them with typical characteristics of a sintering agglomeration process occurring during ash formation. It is interesting to note that there were no spherical particles, as is usual in fusion processes, for example in the generation of coal fly ash [16]. Fig. 1 presents two SEM images of ash samples taken at two different magnifications. The chemical composition of the ash determined by EDS is shown in Fig. 2. The analysis indicates the presence of significant percentages of Mg, Ca and K, while the contents of Al and Si are relatively low. These elements are highly beneficial for the production of dense bodies at the normal temperatures used in the traditional ceramic and refractory industries, constituting their oxides the base material of most of those ceramic materials.

The humidity content of the ash was determined on three samples, calculating the total weight loss occurred until a constant weight was recorded upon heat treatment at 100 °C. The average weight loss was determined to be 1.35%.

The weight loss was also investigated by calcination of samples of grain size <600 μm at 800 °C for 3 h. Ash samples of different weights, chosen randomly from the total amount of the available material, were considered. The values of weight loss measured were small, all below 3%, resulting in an average of 2.73%. This result leads to the conclusion that the material can be used directly to form green bodies, since they will not suffer a significant reduction in volume that would result in large deformation or breaking of the pieces during sintering, if the heat treatment is carried out at an adequate heating rate.

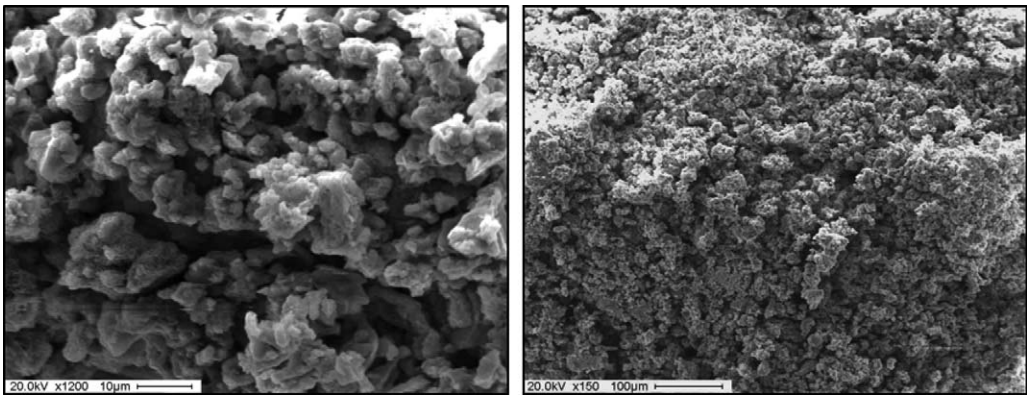

Fig. 1. SEM morphology of the investigated ash at different magnifications.

Element	Weight %
C	21,4
O	40,5
Mg	15,6
Al	1,1
Si	4,0
P	4,8
Cl	0,1
K	4,6
Ca	7,9

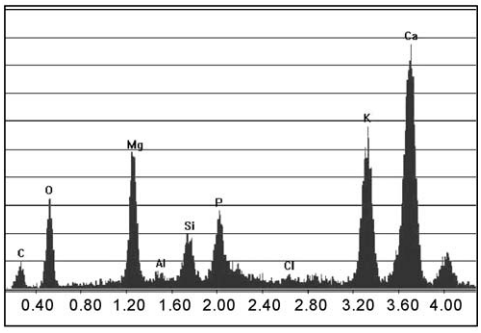

Fig. 2. Elemental analysis of the ash by EDS.

The particle size distribution of the ash was determined by the sieving method on two different samples, one containing environment humidity, as extracted from deposits, and the other being dry ash, e.g. treated at 100 °C for 24 h. The results are shown in Fig. 3. A significant percentage of large particles was observed in both samples, so that a grinding and particle separation process is considered necessary before further processing (compaction operation). Given the low moisture content of these samples similar particle size distributions in the dry and humid ashes are observed, with values somewhat higher in the case of the wet material. These results indicate that it is possible to use the ash in as-received condition from the deposition area without the requirement of a calcination step. However a selection of particle size to achieve structurally robust green bodies will be necessary.

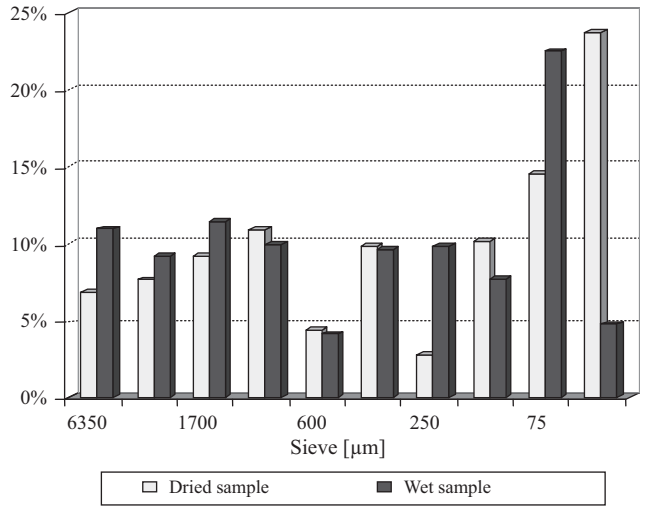

Fig. 3. Particle size distribution of ash samples in wet and dry conditions.

Preliminary tests were conducted on samples fabricated from ash without additional material (particle size <250 μm), producing green bodies with a humidity of about 5%.

Analyzing the ternary equilibrium diagrams of the major oxides present in these mixtures, it is possible to estimate theoretically that excessively high sintering temperatures will be required, due to the low silica content, and thus lack of viscous flow densification which would result impracticable and not economically viable on an industrial scale. This fact was experimentally corroborated as green bodies were heat treated at temperatures as high as 1600 °C without achieving satisfactory densification by sintering.

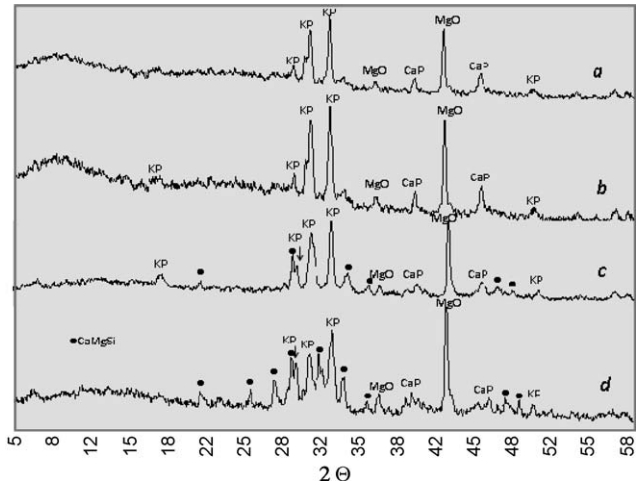

Fig. 4. X-ray diffraction patterns of investigated materials: (a) starting ash, dried at 100 °C, and ash heat-treated at: (b) 1300 °C, (c) 1500 °C, (d) 1600 °C.

While the ash compacts treated at high temperatures did not reach the sintering temperature, chemical transformations and possible reactions of their components could be detected. To analyze these reactions, powders of the used material (ash) treated at different temperatures were analyzed by X-ray diffraction, and results are shown in Fig. 4. The X-ray diffraction spectrum (a) corresponds to the starting material used to form the green bodies, while spectra (b), (c) and (d) correspond to the samples treated at 1300, 1500 and 1600 °C.

As shown in Fig. 4, spectra (a) and (b) are very similar, which is explained because sample (a) corresponds to ash as available in the deposits (only dried at 100 °C), i.e. it has been produced by the burning process of husks of sunflower seeds at temperatures close to 1200–1300 °C. On the other hand, sample (b) corresponds to the same ash after a secondary heat treatment to 1300 °C. Several compounds such as magnesium oxide (MgO), potassium phosphate ($K_5P_3O_{10}$), labelled KP, and calcium phosphate ($Ca_3(PO_4)_2$), CaP, can be identified.

In diffraction patterns (c) and (d), the formation of a new crystalline phase identified as calcium–magnesium silicate ($Ca_2Mg(Si_2O_7)$), labelled CaMgSi in the figure, was detected. This phase is originated from the amorphous silicate glassy phase present in the samples, which can be detected in spectra (a) and (b) by the presence of a bump at low 2θ ($2\theta = 8°$). These characteristic bumps at low angles are lower in samples (c) and (d), due to consumption of the amorphous silicate for the formation of the mixed silicate crystalline phase.

From the results of the different characterization techniques used, it is concluded that it is not possible to obtain dense sintered bodies from ash compacts at temperatures lower than 1600 °C if no additives are added to reduce the sintering temperature. For this reason, mixtures of ash (<250 μm) and powdered cullet (soda-lime) glass of particle size <75 μm were prepared. Fig. 5 shows the EDS analysis of the cullet glass used. This material has a high content of SiO_2 and Na, which should lead to a marked reduction of the sintering temperature of the mixture. Furthermore, given the original composition of the ash, the chance of emergence of new phases by reactions with those already present in the ash noticeably increases.

Preliminary experiments were carried out with blocks of dimensions 70 mm × 40 mm × 10 mm containing approximately 30 wt% of cullet glass and subjected to heat treatment at 1300 °C for 3 h. Fig. 6 shows the image of a green body used in these preliminary tests. Heat treatment resulted in structural components with a substantial degree of sintering which maintained their original form, without the presence of cracks and exhibiting a little increase of the dimensions of fired samples in comparison with those of the green bodies. Based on this result, samples with addition of cullet glass were fabricated and different heat treatments were applied in order to determine the best conditions to produce compact bodies from ash/glass cullet combinations. Weight percentages of 30%, 40% and 50% cullet glass were used. These samples will be identified onwards as M30, M40 and M50, respectively.

The experiments for determining the sintering temperature of these mixtures were carried out by heat treatments at intervals of 25 °C. The optimal temperatures were found to be 1400 °C, 1300 °C and 1250 °C for samples M30, M40 and M50, respectively. That is, the sintering temperatures of the compacts were within the range of temperatures used in the

Oxides	Weight %
Na_2O	18,94
MgO	3,93
Al_2O_3	3,71
SiO_2	62,67
K_2O	0,86
CaO	6,77
FeO	3,12

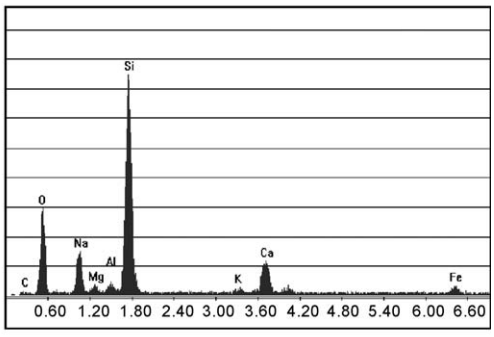

Fig. 5. EDS analysis of cullet glass used (soda-lime composition).

Fig. 6. Green body obtained by uniaxial pressing of ash mixed with powdered cullet glass (dimensions: 70 mm × 40 mm × 10 mm).

conventional firing of traditional ceramics and refractory materials.

The porosity of sintered bodies was determined according to the IRAM local standard (IRAM 12510) for this kind of material. The porosity values were relatively high and similar to each other; 54.8%, 54.5% and 54.4% for samples M30, M40 and M50, respectively. These porosity values allow classifying the obtained products within the typology of alleviating bricks, taking into account the local classification standards.

In spite of the similarity in the values of porosity, pore sizes were seen to be different, as observed in Fig. 7, where optical microscopy photographs are shown. The M50 sample has pores considerably smaller than those of the other two samples studied. Microstructural characterization of these samples by optical microscopy shows distinct areas identified as: granular, platelet, matrix and baton structure. The proportion of each area in the samples varies considerably. The micrographs of fracture surfaces shown in Fig. 8 exemplify the most abundant zone in each sample. It is possible to observe significant presence of granular areas in sample M30, while in sample M40 the formation of a platelet microstructure in a vitreous matrix is observed. In sample M50, on the other hand, structures like interlaced batons are observed. Such formations usually result in a reinforcement of the material, leading to improved fracture toughness of the glass/crystal material [19].

These different structural areas have been also studied by scanning electron microscopy, and chemically analyzed by EDS. The characterization of granular areas can be seen in Fig. 9, where a SEM micrograph of these areas, mainly present in sample M30, is shown. The corresponding chemical analyses at grain boundaries and at the interior of a grain are also presented. As observed in the analysis spectra, grain boundary areas are rich in K, Al and Mg, while the interior of the grain shows a higher concentration of Ca and P. An elemental mapping reflecting clearly the distribution of the different elements in the material structure is also shown in Fig. 9. The areas of formation of platelets, mainly observed in sample M40, were also studied by these techniques and results are shown in Fig. 10. In the chemical analysis of the platelets and the matrix that contains them, Si is identified as the main component in both areas. The platelets also contain a significant amount of Ca and Mg while the matrix has a high percentage of K. These results can be seen in the mapping of these elements included in Fig. 10.

Fig. 11 presents the results of SEM and EDS on sample M50. It is noted the presence of batons and platelets, contained in a matrix of similar characteristics to those observed in other samples, mainly composed of Si and K. The chemical analyses conducted on these areas show similar components, Ca and Si,

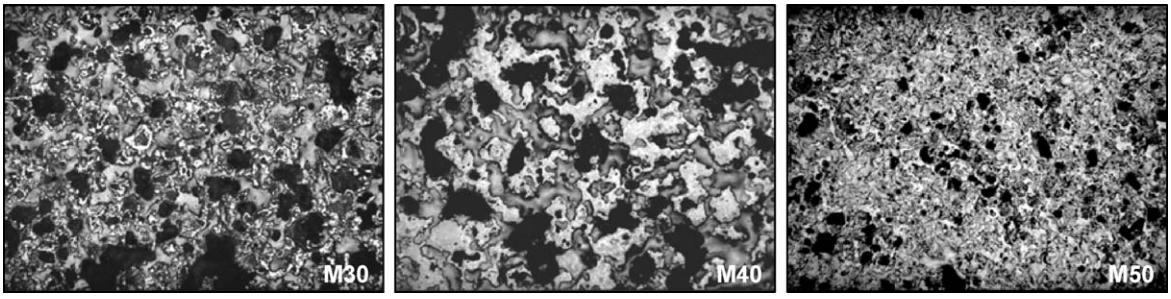

Fig. 7. Optical microscopy images of sintered ash/cullet glass bodies with different glass concentration (samples M30, M40 and M50). Magnification: ×50.

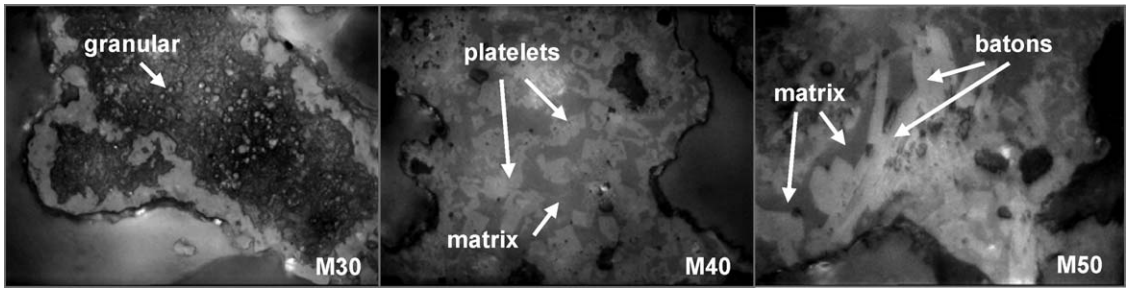

Fig. 8. Optical microscopy images of fracture surfaces of samples M30, M40 and M50 showing typical microstructural features. Magnification: ×500.

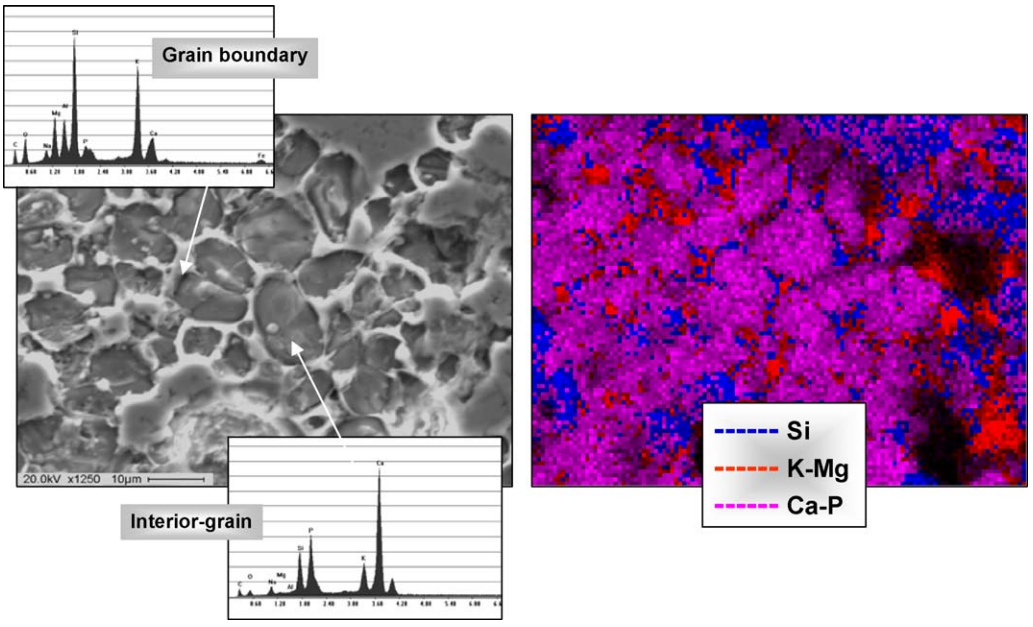

Fig. 9. SEM–EDS characterization of granular areas in sample M30.

with a greater Mg proportion in the platelets than in the batons, where the percentage of Mg is very low. It is interesting to note that some structures that seem like small chains are situated inside the pores in sample M50. The chemical analysis of these structures reflects a high content of P, as observed by SEM–EDS studies on sample M50, shown in Fig. 12. This structural form is however absent in samples M30 and M40.

X-ray diffraction (XRD) patterns of powdered samples M30, M40 and M50 are shown in Fig. 13, where only new phases formed are identified. Sample M30 shows some small peaks detected in the sunflower ash analysis, presented in Fig. 4, corresponding to magnesium oxide (MgO), and calcium phosphate ($Ca_3(PO_4)_2$). In this sample, the mixture between the original ash and cullet glass and the heat treatment applied made possible the formation of new phases, which are identified as calcium magnesium silicate ($CaMgSiO_4$), present in major proportion, and calcium magnesium potassium phosphate ($Ca_9MgK(PO_4)_7$). This result agrees with the elemental analysis carried out by EDS on the boundaries and interior of grains in areas called ‘‘granular’’ (Fig. 9). In the XRD patterns for samples M40 and M50 it is possible to observe that the first mentioned phase is present in a lower proportion, probably due to the formation of a vitreous phase which constitutes the matrix phase (see ‘‘matrix’’ analysis in Fig. 10). In these samples also a new silicate phase is detected. Its identification corresponds to a calcium magnesium silicate

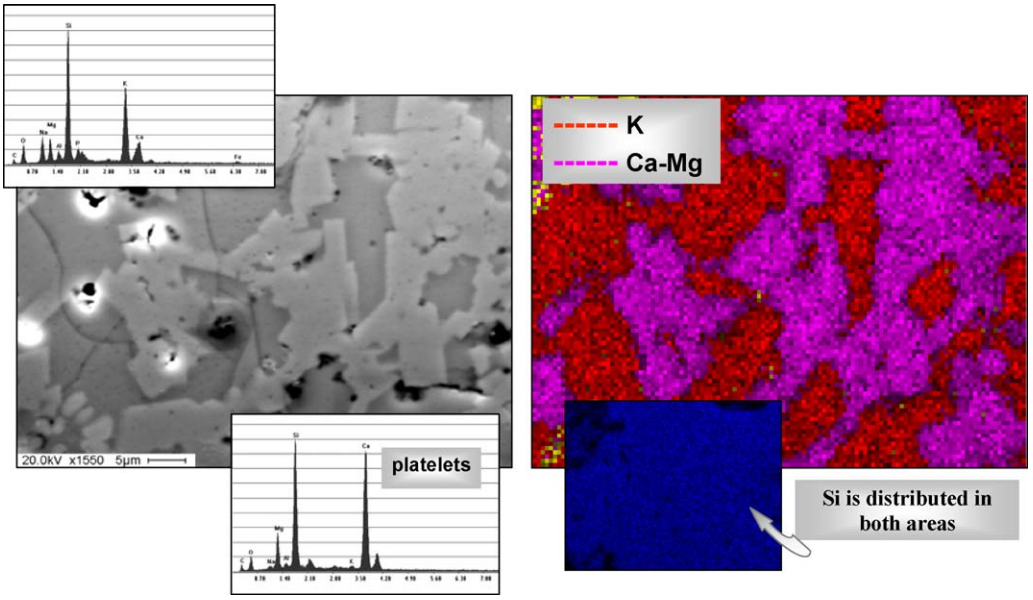

Fig. 10. SEM–EDS characterization of microstructural features (platelet morphology) in sample M40.

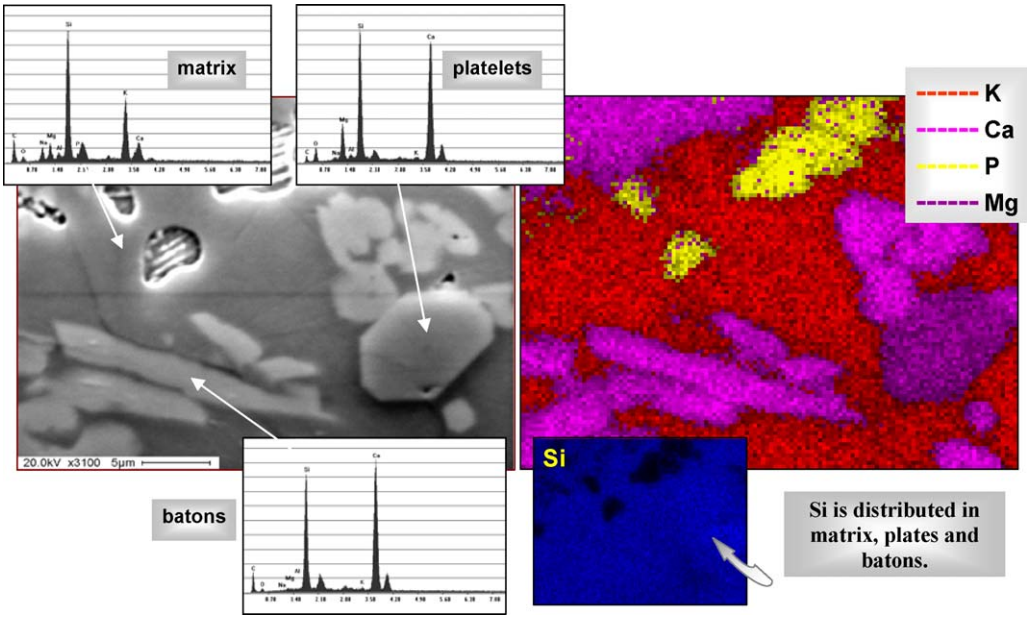

Fig. 11. SEM–EDS characterization of microstructural features (batons-platelet areas) in sample M50.

structure of the type of akermanite ($Ca_2Mg(Si_2O_7)$). This phase can contain also small quantities of sodium, aluminium and iron. In order to analyze these results in the light of the data obtained from SEM and EDS studies, it is possible to conclude that the ''platelets'' detected in more proportion in samples M40 and M50 are constituted by akermanite structure. The batons form can be ascribed to orthorhombic calcium silicate which has only one strong peak in its diffraction pattern, located at 2Θ values in the range of those of the other majority phases ($2\Theta \sim 31^\circ$). In relation to the small chain structure observed only in sample M50 (Fig. 12), it is speculated that this formation is the same compound identified as $CaMgK(PO_4)_7$ in the other two samples, but with a different arrangement. This explanation is plausible because there is no other phosphate crystalline phase detected in the corresponding XRD pattern of this sample (M50). All mentioned crystalline structures correspond to new phases formed during the heat treatment, indicating that densification and microstructure formation is not a simple viscous flow sintering process but also it involves chemical reactions and formation of new crystalline structures. The in situ development of these crystalline structures with different, well-defined morphologies, as investigated here, is relevant considering their possible reinforcing effect in the final products, which could attain mechanical properties relevant for applications in the construction industry or other uses.

As a first attempt at characterizing the mechanical response of the materials the Vickers microhardness (Hv) of the different structures present in the studied samples; granular, platelet, matrix and batons, was determined. The results were similar in all samples. Fig. 14 shows a SEM photograph of sample M50, where all mentioned structures with the corresponding Hv values can be observed.

In sample M50 it is possible to anticipate relatively high fracture toughness, as the material exhibits better defined indentations and no cracks in comparison to the other samples. This behaviour can be explained by the presence of a larger

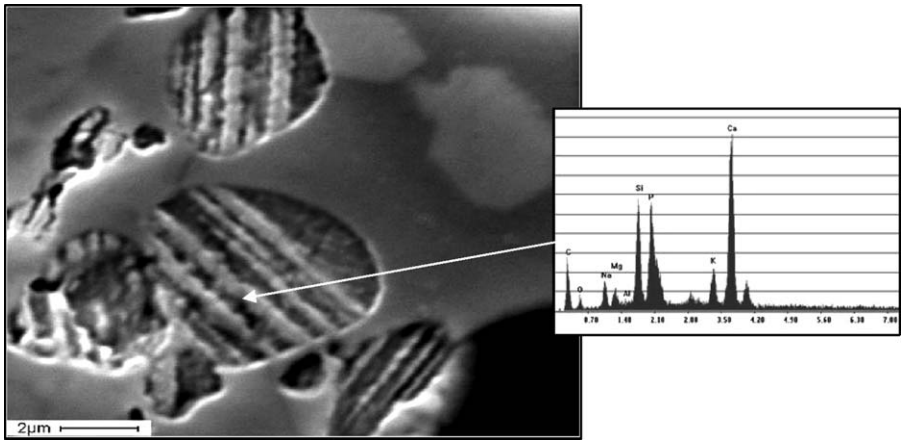

Fig. 12. SEM–EDS characterization of microstructural features in sample M50 showing ''small chains'' morphology.

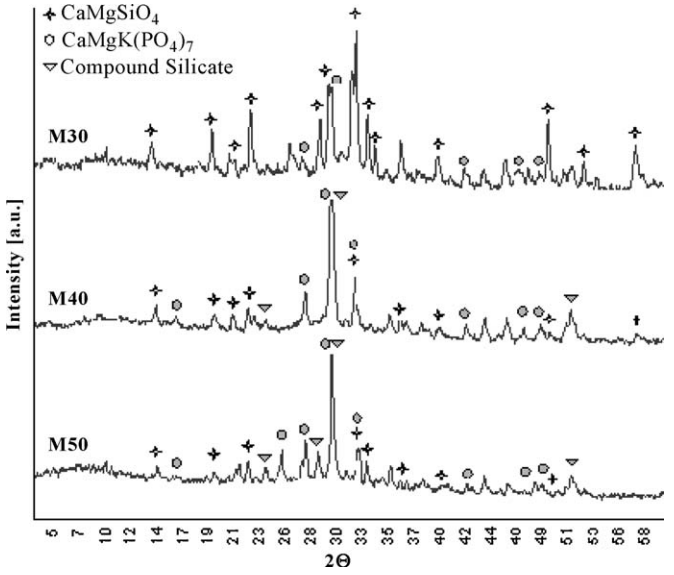

Fig. 13. XRD patters of powdered samples M30, M40 and M50.

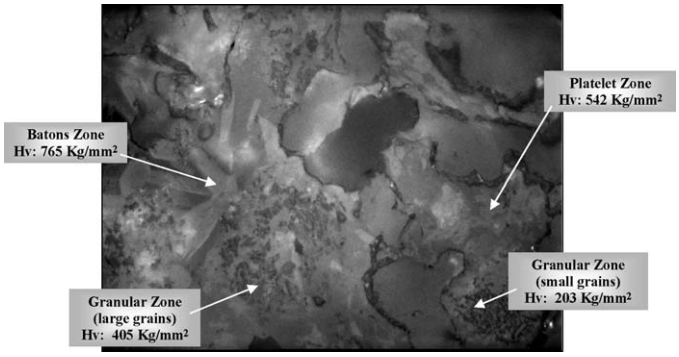

Fig. 14. Vickers microhardness values taken on areas containing different microstructural morphologies: platelets, batons and granular structure, present in sample M50.

proportion of the batons-type crystals and the smaller size of pores. It is also possible that the presence of structures in ''small chains'' morphology (Fig. 12) will contribute to reinforce the material, as crystals with high aspect ratio are effective in promoting toughening mechanisms such as crack deflection in glass/crystal composites [19].

4. Conclusions

The ash produced by burning husks of sunflower seeds has been characterized and the feasibility for its use to develop new glass/crystal materials for possible applications in the construction industry has been investigated. The results have shown that this waste material can be used for that purpose if it is treated firstly by grinding and particle size separation to eliminate large agglomerates. Powder compacts made from the ash (no additives) present a very high sintering temperature, which would not allow this process to be viable at industrial scale. Experiments conducted with mixtures of the ash and powdered cullet glass in proportions (wt%) of 30%, 40% and 50% showed that it is feasible to use these mixtures for the production of glass/crystalline materials at sintering temperatures compatible with those used in industrial processes (<1400 °C). Materials exhibiting well-defined microstructures with specific crystal morphology and compositions were produced and formation of new phases during the sintering process was investigated. Crystalline phases such as calcium magnesium silicate and calcium magnesium potassium phosphate were identified and their relative content varied depending on the ash/glass cullet ratio. The M50 sample exhibited the most attractive features: lowest sintering temperature (1250 °C), smallest possible pore size and possibly the greatest fracture toughness due mainly to the higher proportion of interlaced structures formed by randomly orientated crystalline batons and small chains structures of high aspect ratio.

Acknowledgements

The authors would like to express their thanks for the financial support provided by ANPCyT (Agencia Nacional de Promoción Científica y Tecnológica), Project PICTN 35672, and by CIC (Comisión Científica de la Provincia de Buenos Aires).

They also thank to Vicentin S.A.I.C. for the discarded material used in this study.

References

[1] C. Yin, L. Rosendahl, S. Kaer, Grate-firing of biomass for heat and power production, Prog. Energy Comb. Sci. 34 (2008) 725–754.
[2] J. Gañán, A. Al-Kassir Abdulla, E. Cuerda Correa, A. Macías-García, Energetic exploitation of vine shoot by gasification processes. A preliminary study, Fuel Process. Technol. 87 (2006) 891–897.
[3] J. González, J. Encinar, J. Canito, E. Sabio, M. Chacón, Pyrolysis of cherry stones: energy uses of the different fractions and kinetic study, J. Anal. Appl. Pyrol. 67 (2003) 165–190.
[4] J. Encinar, J. González, G. Martínez, Energetic use of the tomato plant waste, Fuel Process. Technol. 89 (2008) 1193–1200.
[5] W. Ghani, A. Alias, R. Savory, K. Cliffe, Co-combustion of agricultural residues with coal in a fluidised bed combustor, Waste Manage. 29 (2009) 767–773.
[6] J. Encinar, J. González, G. Martínez, Two stages catalytic pyrolysis of olive oil waste, Fuel Process. Technol. 89 (2008) 1448–1455.
[7] H. Haykiri Acma, S. Yaman, Effect of co-combustion on the burnout of lignite/biomass blends: a Turkish case study, Waste Manage. 28 (2008) 2077–2084.
[8] D. Mohan, C. Pittman Jr., Activated carbons and low cost adsorbents for remediation of tri- and hexavalent chromium from water, J. Hazard. Mater. B137 (2006) 762–811.
[9] A. Nunes, A. Franca, L. Oliveira, Activated carbons from waste biomass: an alternative use for biodiesel production solid residues, Bioresour. Technol. 100 (5) (2009) 1786–1792.
[10] Y. Erel, A. Mathews, Y. Nathan, Potential use of coal ash in the Israel Cement Industry, Cem. Conc. Res. 18 (1988) 503–512.
[11] J. Olek, Dinamic/static modulus of elasticity and Poisson's ratio of flyash concrete, in: A.M. Brandt, V.C. Li, I.H. Marshall (Eds.), Proc. Int. Symp. Brittle Matrix Composites 4, IKE and Woodhead Publ., Warsaw, 1994 pp. 425–436.
[12] S. Tyson, T. Blackstock, Coal combustion fly ash – overview of applications and opportunities in the USA, in: Proc. 211th ACS National Meet, New Orleans, USA, (1996), pp. 587–591.
[13] D. Golden, Research to develop coal ash uses, in: Proc. 9th Int. Ash Use Symp., Orlando, USA, (1991), pp. 69.1–69.23.

[14] S. Vassilev, R. Menendez, M. Diaz-Somoano, M. Martinez-Tarazona, Phase-mineral and chemical composition of coal fly ashes as a basis for their multicomponent utilization. 2. Characterization of ceramic cenosphere and salt concentrates, Fuel 83 (2004) 585–603.
[15] M. Little, V. Adell, A. Boccaccini, C. Cheeseman, Production of novel ceramic materials from coal fly ash and metal finishing wastes, Resour. Conserv. Recy. 52 (11) (2008) 1329–1335.
[16] A. Boccaccini, M. Bücker, J. Bossert, K. Marszalek, Glass matrix composites from coal flyash and waste glass, Waste Manage. 17 (1997) 39–45.
[17] A. Francis, R. Rawlings, R. Sweeney, A. Boccaccini, Crystallization kinetic of glass particles prepared from a mixture of coal ash and soda-lime cullet glass, J. Non-Cryst. Solids 333 (2004) 187–193.
[18] R. Rawlings, J. Wu, A. Boccaccini, Glass-ceramics: their production from wastes. A review, J. Mater. Sci. 41 (2006) 733–761.
[19] R. Todd, A. Boccaccini, R. Sinclair, R. Yallee, R. Young, Thermal residual stresses and their toughening effect in Al_2O_3 platelet reinforced glass, Acta Mater. 47 (1999) 3233–3240.